Promoter unwinding and promoter clearance by RNA polymerase: Detection by single-molecule DNA nanomanipulation

Andrey Revyakin*[†], Richard H. Ebright*[‡], and Terence R. Strick[†§]

*Howard Hughes Medical Institute, Waksman Institute, and Department of Chemistry, Rutgers, The State University of New Jersey, Piscataway NJ 08854; and [†]Cold Spring Harbor Laboratory, Cold Spring Harbor, NY 11724

By monitoring the end-to-end extension of a mechanically stretched, supercoiled, single DNA molecule, we have been able directly to observe the change in extension associated with unwinding of approximately one turn of promoter DNA by RNA polymerase (RNAP). By performing parallel experiments with negatively and positively supercoiled DNA, we have been able to deconvolute the change in extension caused by RNAP-dependent DNA unwinding (with ≈1-bp resolution) and the change in extension caused by RNAP-dependent DNA compaction (with ≈5-nm resolution). We have used this approach to quantify the extent of unwinding and compaction, the kinetics of unwinding and compaction, and effects of supercoiling, sequence, ppGpp, and nucleotides. We also have used this approach to detect promoter clearance and promoter recycling by successive RNAP molecules. We find that the rate of formation and the stability of the unwound complex depend profoundly on supercoiling and that supercoiling exerts its effects mechanically (through torque), and not structurally (through the number and position of supercoils). The approach should permit analysis of other nucleic-acid-processing factors that cause changes in DNA twist and/or DNA compaction.

Transcription initiation involves a series of reactions (1–2): (*i*) RNA polymerase holoenzyme (RNAP) binds to promoter DNA to form an RNAP–promoter closed complex; (*ii*) RNAP unwinds approximately one turn of the promoter DNA to form an RNAP–promoter open complex (in a process referred to as "promoter unwinding"); and (*iii*) RNAP escapes the promoter and enters into productive synthesis of RNA as an RNAP–DNA elongation complex (in a process referred to as "promoter clearance").

We have developed a single-molecule DNA-nanomanipulation approach that enables us to detect and characterize promoter unwinding and promoter clearance by RNAP. Our approach uses an experimental setup originally developed for analysis of DNA polymer physics (Fig. 1*A* and refs. 3–5). In this experimental setup, a double-stranded DNA molecule containing a single promoter site is attached at one end, through multiple linkages, to a paramagnetic bead, and at the other end, through multiple linkages, to a glass surface; the DNA is torsionally constrained and mechanically stretched between the bead and the glass surface by application of a pair of magnets above the DNA helix axis; and the distance between the bead and the glass surface (which reflects the DNA end-to-end extension, l) is monitored in real time by using videomicroscopy. Upon rotation of the pair of magnets, the bead is rotated in lock-step register, superhelical turns are introduced into the torsionally constrained DNA molecule in lock-step register, supercoils are formed, and, correspondingly, l is changed. With this experimental setup, it readily is possible to construct an experimental calibration curve relating l to the number of clockwise or counterclockwise rotations of the pair of magnets, and thus to the number of negative or positive superhelical turns (Fig. 1*B*; refs. 3–5). Over a broad range of negative or positive supercoiling, l changes linearly with the number of negative or

positive superhelical turns, with, under our conditions, a change in l of 56 ± 5 nm per superhelical turn (Fig. 1*B*).

Fig. 1 *C* and *D* shows how we use this experimental setup to detect promoter unwinding by RNAP. Conservation of linking number (Lk), according to the established relationship $Lk = Tw + Wr$ (6), implies that in a torsionally constrained DNA molecule a change in twist (Tw; unwinding) must be compensated by an equal, but opposite, change in writhe (Wr; number of supercoils). With a negatively supercoiled DNA molecule, unwinding of approximately one turn of promoter DNA by RNAP must result in a compensatory loss of approximately one negative supercoil and, correspondingly, an increase in l of ≈56 nm ($\Delta l_{obs,neg}$; Fig. 1*C*). With a positively supercoiled DNA molecule, unwinding of approximately one turn of promoter DNA by RNAP must result in a compensatory gain of approximately one positive supercoil and, correspondingly, a decrease in l of ≈56 nm ($\Delta l_{obs,pos}$; Fig. 1*D*). Thus, our approach couples RNAP-dependent promoter unwinding to movement of the bead. This results in an immense amplification of signal: converting a subnanometer scale, effectively undetectable, change in local DNA geometry, to a tens-of-nanometer scale, readily detectable, change in the position of the bead.

Methods

DNA Fragments. *lacCONS*-4kb and *rrnB*P1–4kb are 4-kb G/C-rich (67% G/C) DNA fragments that contain centrally located single copies of, respectively, the *lacCONS* promoter (7, 8) and the *rrnB* P1 promoter (23). *lacCONS*-4kb and *rrnB*P1–4kb were prepared, attached to beads, attached to glass surfaces, and calibrated as described for *rrnB*P1–4kb in ref. 5.

Data Collection. Unless noted otherwise, reaction mixtures contained 0.5 nM RNAP (Epicentre) and negatively supercoiled, mechanically stretched, DNA molecule *lacCONS*-4kb or *rrnB*P1–4kb (ref. 5; $\sigma = -0.018$; extending force = 0.3 pN), or 5 nM RNAP (Epicentre) and positively supercoiled, mechanically stretched, DNA molecule *lacCONS*-4kb or *rrnB*P1–4kb (ref. 5; $\sigma = 0.018$; extending force = 0.3 pN), in transcription buffer (25 mM Hepes·NaOH, pH 7.9/100 mM NaCl/10 mM MgCl$_2$/0.1% Tween 20/0.1 mg/ml BSA/3 mM 2-mercaptoethanol) at 34°C. Reactions were initiated by introduction of transcription buffer containing RNAP by flow (1 ml; 1 min), followed by cease of flow and data collection. Reactions were terminated, and the DNA molecule was recycled for further experiments, by application of an extending force and introduc-
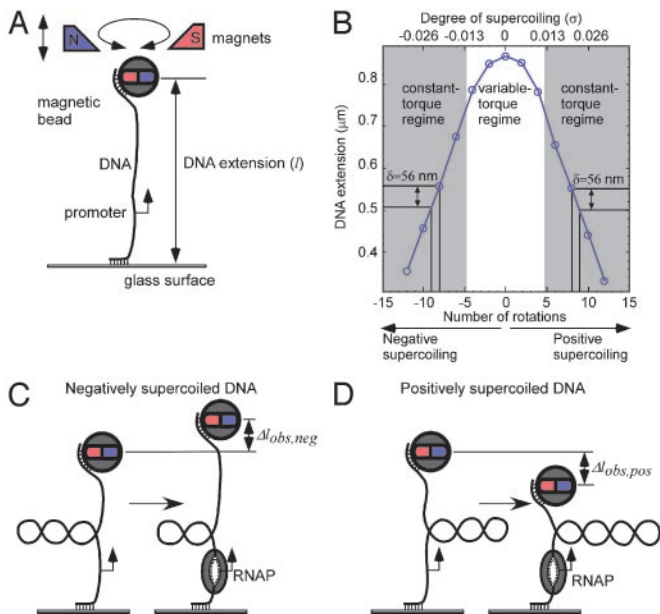

Fig. 1. Experimental approach. (*A*) Experimental setup. A double-stranded 4-kb DNA molecule containing a single promoter is tethered at one end, through multiple linkages, to a paramagnetic bead, and at the other end, through multiple linkages, to a glass surface. The DNA is torsionally constrained and mechanically stretched between the bead and the glass surface by application of a pair of magnets above the DNA helix axis. The distance between the bead and the surface, which reflects the DNA end-to-end extension (*l*), is monitored in real time by videomicroscopy. Upon rotation of the pair of magnets, the bead is rotated in lock-step register, superhelical turns are introduced into the DNA in lock-step register, plectonemic supercoils are formed, and, correspondingly, *l* is changed. (*B*) Calibration of *l* vs. number of superhelical turns. Over a broad range of positive and negative supercoiling, there is a linear relationship between *l* and the number of superhelical turns, with a change in *l* (δ) of 56 ± 5 nm per superhelical turn. (*C* and *D*) Detection of promoter unwinding. According to the relationship $Lk = Tw + Wr$ (6), in a torsionally constrained DNA molecule with constant linking number (*Lk*), a change in twist (*Tw*; unwinding), must be compensated by an equal, but opposite, change in writhe (*Wr*; number of supercoils). With negatively supercoiled DNA, unwinding of approximately one turn of promoter DNA by RNAP must result in a compensatory loss of approximately one negative supercoil and, correspondingly, an increase in *l* ($\Delta l_{obs,neg}$). With positively supercoiled DNA, unwinding of approximately one turn of promoter DNA by RNAP must result in a compensatory gain of approximately one positive supercoil and, correspondingly, a decrease in *l* ($\Delta l_{obs,pos}$).

tion of at least five positive supercoils, followed by introduction of transcription buffer (3 ml; 15 min).

Data Analysis: DNA Unwinding and DNA Compaction. DNA unwinding has opposite effects on *l* in experiments with negatively and positively supercoiled DNA (increases *l* with negatively supercoiled DNA; decreases *l* with positively supercoiled DNA), whereas DNA compaction has equivalent effects on *l* in experiments with negatively and positively supercoiled DNA (decreases *l* with both negatively and positively supercoiled DNA). Therefore, effects of unwinding and compaction can be deconvoluted from data with negatively and positively supercoiled DNA by use of simple algebra (Fig. 2*C* and Fig. 5, which is published as supporting information on the PNAS web site; see ref. 5). From experimental time traces with data averaged by using a 1-s window (red points in Fig. 2), extents of DNA unwinding can be determined to within ±3 bp, and extents of DNA compaction can be determined to within ±20 nm; from experimental time traces with data averaged by using a 20-s window, extents of unwinding can be determined to within ±

1 bp, and extents of compaction can be determined to within ±5 nm.

Data Analysis: T_{wait} and $T_{unwound}$. Histograms of observed values of T_{wait} and $T_{unwound}$ were prepared from ≥100 individual unwinding/rewinding events in raw time traces. Histograms displayed single-exponential distributions, with mean equal to standard deviation, allowing determination of mean values of T_{wait} and $T_{unwound}$ as half-lives of distributions (Fig. 3*A*).

Results and Discussion

We have performed experiments using *Escherichia coli* RNAP and the consensus promoter *lacCONS* (7, 8). Fig. 2 *A* and *B* document detection of formation of the unwound complex in experiments with negatively and positively supercoiled DNA, respectively. With negatively supercoiled DNA, under conditions where, based on conventional assays, the RNAP–promoter open complex is expected to be stable and effectively irreversible, experimental single-molecule traces of *l* vs. time reveal single, abrupt, effectively irreversible, increases in DNA extension ($\Delta l_{obs,neg}$ = 50 ± 5 nm; Fig. 2*A*; see also Fig. 6*A*, which is published as supporting information on the PNAS web site). With positively supercoiled DNA, under conditions where, based on conventional assays, the RNAP–promoter open complex is expected to be unstable and reversible, experimental single-molecule traces of *l* vs. time reveal cycles of abrupt decreases in *l* ($\Delta l_{obs,pos}$ = 80 ± 5 nm) followed by abrupt increases in *l*, returning to the initial state ($\Delta l_{obs,pos}$ = 80 ± 5 nm; Fig. 2*A*; see also Fig. 6*B*). Extensive control experiments establish that the observed transitions correspond to single promoter-unwinding and promoter-rewinding events. Thus: (*i*) no events are observed in the absence of RNAP; (*ii*) no events are observed in the absence of the initiation factor σ; (*iii*) no events are observed in the absence of a promoter; (*iv*) one, two, or three levels of events are observed with DNA molecules containing, respectively, one, two, or three promoters; (*v*) no events are observed at low temperatures (which are known to prevent formation of open complexes refs. 1 and 2); (*vi*) events are prevented by prior addition of heparin (which is known to prevent formation of open complexes; ref. 9); and (*vii*) events are not affected by subsequent addition of heparin (which is known not to affect open complexes once formed; ref. 9) (Figs. 7–11, which are published as supporting information on the PNAS web site, and additional data not shown).

The experimental time traces yield four observables. The first observable is the number of states, which reflects the number of unwinding intermediates in promoter unwinding (Fig. 2 *A* and *B*). The experimental time traces show only two states: an initial state and a final state, with abrupt, sharp transitions between them. Thus, there are no unwinding intermediates in promoter unwinding, at least none with lifetimes equal to or greater than the temporal resolution of the analysis (≈1 s).

The second observable is the amplitude of the transition between the initial and final states ($\Delta l_{obs,neg}$ with negatively supercoiled DNA; $\Delta l_{obs,pos}$ with positively supercoiled DNA; Fig. 2 *A* and *B*). The amplitude of the transition is a function of the extent of DNA unwinding, and of the extent of DNA compaction (arising from DNA wrapping and/or DNA bending). From the experimental time traces obtained with negatively supercoiled DNA and with positively supercoiled DNA, we are able to deconvolute the extent of DNA unwinding and the extent of DNA compaction (Figs. 2*C* and 5). The inferred extent of unwinding is 1.2 ± 0.1 turns, which is equivalent to 13 ± 1 bp, which corresponds within experimental error to the extent of unwinding defined by DNA footprinting (1, 2, 10). The inferred extent of compaction is 15 ± 5 nm, which corresponds within experimental error to the extent of compaction defined by
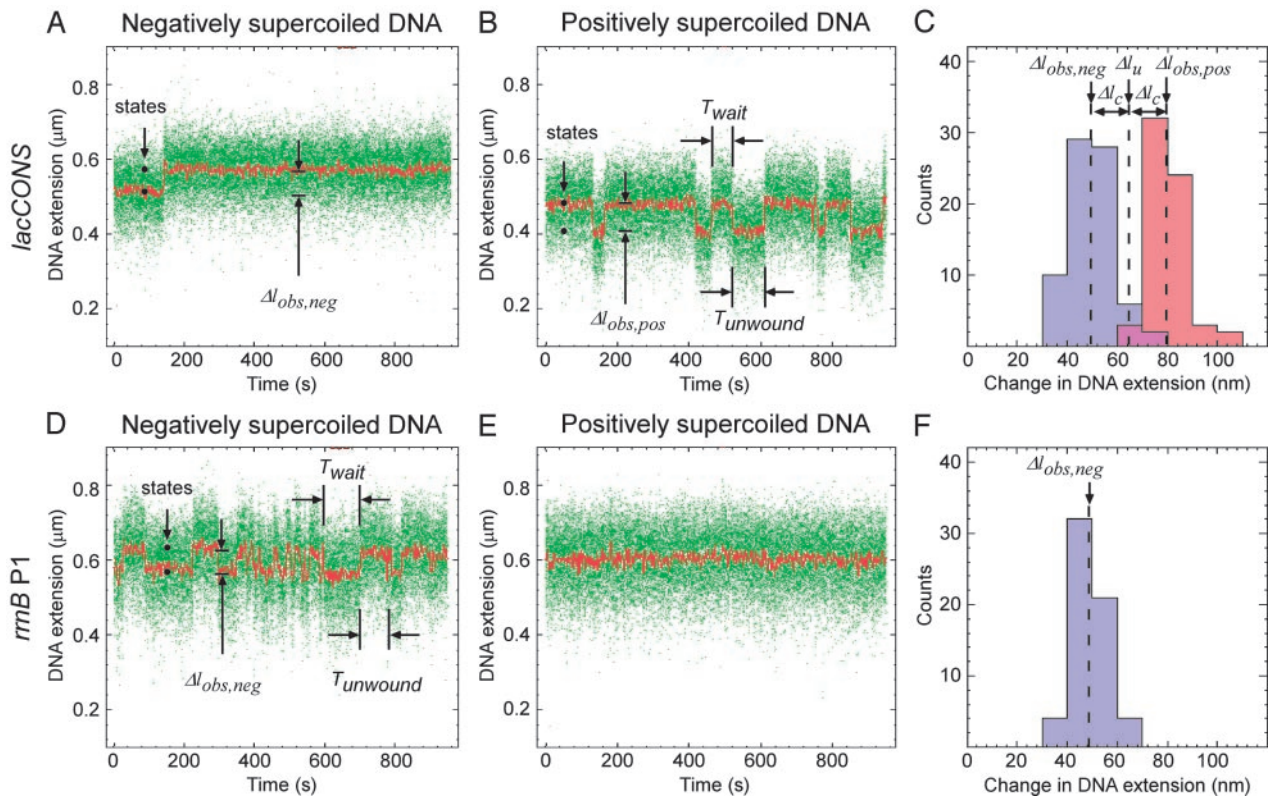
Fig. 2. Detection of promoter unwinding. (*A* and *B*) Single-molecule traces of DNA extension vs. time for interaction of RNAP with a consensus promoter, as assessed with negatively supercoiled DNA (*A*; $\sigma = -0.018$; stable, effectively irreversible, promoter unwinding) and with positively supercoiled DNA (*B*; $\sigma = 0.018$; unstable, reversible promoter unwinding). Green points, raw data obtained at video rate (30 frames per s); red points, averaged data (1-s window); $\Delta l_{obs,neg}$, transition amplitude with negatively supercoiled DNA; $\Delta l_{obs,pos}$, transition amplitude with positively supercoiled DNA; T_{wait}, time interval between a rewinding event and the next unwinding event; $T_{unwound}$, time interval between an unwinding event and the next rewinding event. (*C*) Histograms of $\Delta l_{obs,neg}$ (blue) and $\Delta l_{obs,pos}$ (red). The change in *l* attributable to DNA unwinding (Δl_u) and the change in *l* attributable to DNA compaction arising from wrapping and/or bending (Δl_c) are calculated as $\Delta l_u = (\Delta l_{obs,neg} + \Delta l_{obs,pos})/2$ and $\Delta l_c = (\Delta l_{obs,pos} - \Delta l_{obs,neg})/2$. The extent of unwinding (ΔTw) is calculated as $\Delta Tw = \Delta l_u/\delta$. (See Fig. 5; see also discussion in ref. 5.) (*D–F*) As in *A–C*, but with the *rrnB* P1 promoter (unstable, reversible promoter unwinding with negatively supercoiled DNA; no promoter unwinding with positively supercoiled DNA).

scanning probe microscopy (refs. 11 and 12 and C. Rivetti, N. Naryshkin, E. Kortkhonjia, and R.H.E., unpublished data).

The third observable is the time interval between unwinding events (T_{wait}; Figs. 2 *A* and *B* and 3*A*). T_{wait} is a function of the rate of formation of the unwound complex. From experimental time traces determined at a series of RNAP concentrations (1–30 nM), using tau-plot analysis (13), we are able to deconvolute T_{wait} into the equilibrium-binding constant for formation of closed complex (K_B) and the rate constant for isomerization of closed complex to yield unwound complex (k_2) in the standard kinetic scheme (Fig. 3*B*):

$$R+P \underset{k_{-2}}{\overset{K_B \quad\quad k_2}{\rightleftarrows \; RP_c \; \rightleftarrows}} RP_o. \quad\quad [1]$$
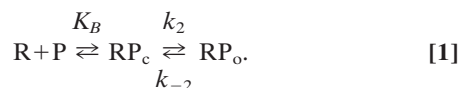
The inferred values of K_B (1×10^7 M^{-1}) and k_2 (0.3 s^{-1}) are consistent with expectation based on conventional experiments (14–17).

The fourth observable is the time interval between an unwinding event and the subsequent rewinding event ($T_{unwound}$; Figs. 2 *A* and *B* and 3*A*). $T_{unwound}$ directly yields the lifetime of the unwound state and the rate constant for rewinding (k_{-2}). As expected, $T_{unwound}$ is independent, within experimental error, of RNAP concentration (Fig. 3*B*). The inferred value of k_{-2} is 0.03 s^{-1}, consistent with expectation based on conventional experiments (14–17).

To assess effects of supercoiling, we performed parallel experiments at superhelical densities of 0.008, 0.011, 0.013, 0.019, and 0.024 [where superhelical densities of 0.008, 0.011, and 0.013 are in the variable-torque regime (where torque increases with increasing superhelical density), and superhelical densities of 0.019 and 0.024 are in the constant-torque regime (where torque is constant with increasing superhelical density) (ref. 18; Figs. 1*B* and 3*C*)]. In the variable-torque regime, T_{wait} increases with increasing superhelical density (4-fold increase for an increase in superhelical density of 0.005), and $T_{unwound}$ decreases with increasing superhelical density (4-fold decrease for an increase in superhelical density of 0.005). Thus, in the variable-torque regime, the ratio $T_{wait}/T_{unwound}$ changes by fully a factor of 16 for a change in superhelical density of 0.005. We conclude that, in the variable-torque regime, supercoiling affects the rate of formation of the unwound complex, the stability of the unwound complex, and, profoundly, the ratio of times in the unwound and wound states (see refs. 14–17). In contrast, in the constant-torque regime, T_{wait} and $T_{unwound}$ are constant. Based on the supercoiling dependence of T_{wait} and $T_{unwound}$ in the variable-torque regime and supercoiling independence of T_{wait} and $T_{unwound}$ in the constant-torque regime, we conclude that effects of supercoiling on promoter unwinding are manifest mechanically (i.e., through changes in torque), and not structurally (i.e., through changes in number and positions of supercoils; hypothesis in refs. 19 and 20). [In this work, where extending force is constant and *l* is variable, the transition
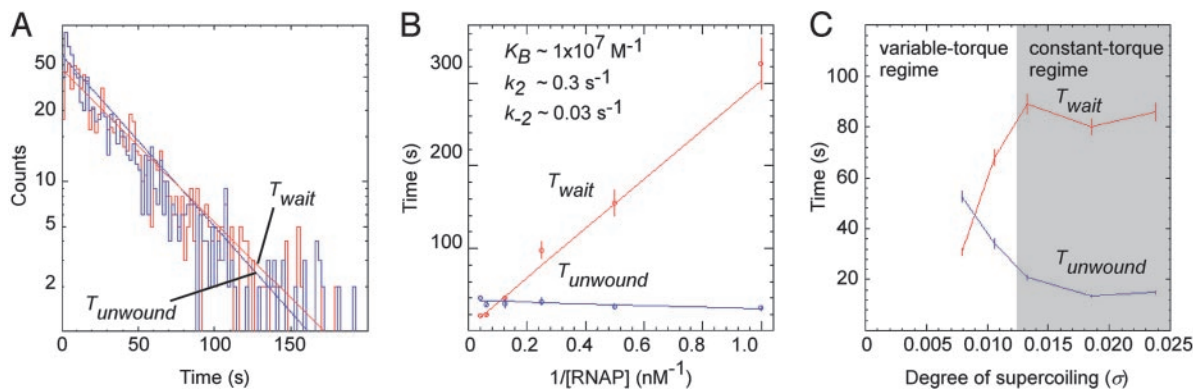
Fig. 3. Kinetics and supercoiling-dependence of promoter unwinding. (*A*) Histograms of T_{wait} and $T_{unwound}$ (consensus promoter, positively supercoiled DNA; $\sigma = 0.018$; $n = 1{,}127$ events). (*B*) Tau plot (13) of values of T_{wait} and $T_{unwound}$ measured at a series of RNAP concentrations (consensus promoter, positively supercoiled DNA; $n \geq 100$ events per RNAP concentration). K_B, k_2, and k_{-2}, are, respectively, the equilibrium constant for formation of closed complex, the rate constant for unwinding, and the rate constant for rewinding in the standard kinetic scheme (refs. 1, 2, and 13; see Eq. **1**). The slope and *y* intercept of the tau plot of T_{wait} yields $(K_B k_2)^{-1}$ and $(k_2)^{-1}$; the *y* intercept of the tau plot of $T_{unwound}$ yields $(k_{-2})^{-1}$. (*C*) Supercoiling-dependence of T_{wait} and $T_{unwound}$ (consensus promoter, positively supercoiled DNA; $\sigma = 0.008$ to 0.024; $n \geq 100$ events per σ value). The variable-torque and constant-torque regimes are defined based on the nonlinear and linear regimes of the experimental calibration curve in Fig. 1*B* (see ref. 18). Torque, $|\Gamma|$, is estimated to be 4.2, 4.4, 4.6, 5.0, and 5.0 pN nm for superhelical densities of 0.008, 0.011, 0.013, 0.019, and 0.024, respectively (refs. 4, 18, and 21 and T.R.S., unpublished results). The magnitude of the supercoiling dependence in the variable-torque regime is consistent with a simple Arrhenius-law model in which torque biases the free energy of promoter unwinding/rewinding (see ref. 26).

between variable-torque and constant-torque regimes occurs at relatively low torque, achieved at relatively low negative or positive superhelical densities ($|\Gamma| \approx 5$ pN nm; $|\sigma| \approx 0.014$; Figs. 1*B* and 3*C*) (4, 18, 21). *In vivo*, where extending force is variable and *l* is constant, the transition between variable- and constant-

torque regimes is expected to occur only at high torque, achieved only at high negative or positive superhelical densities ($|\Gamma| \geq 15$ pN nm; $|\sigma| \geq 0.06$) (4, 17, 18, 21, 22). Therefore, *in vivo*, T_{wait} and $T_{unwound}$ are expected to vary with supercoiling across essentially the full physiological range of supercoiling.]
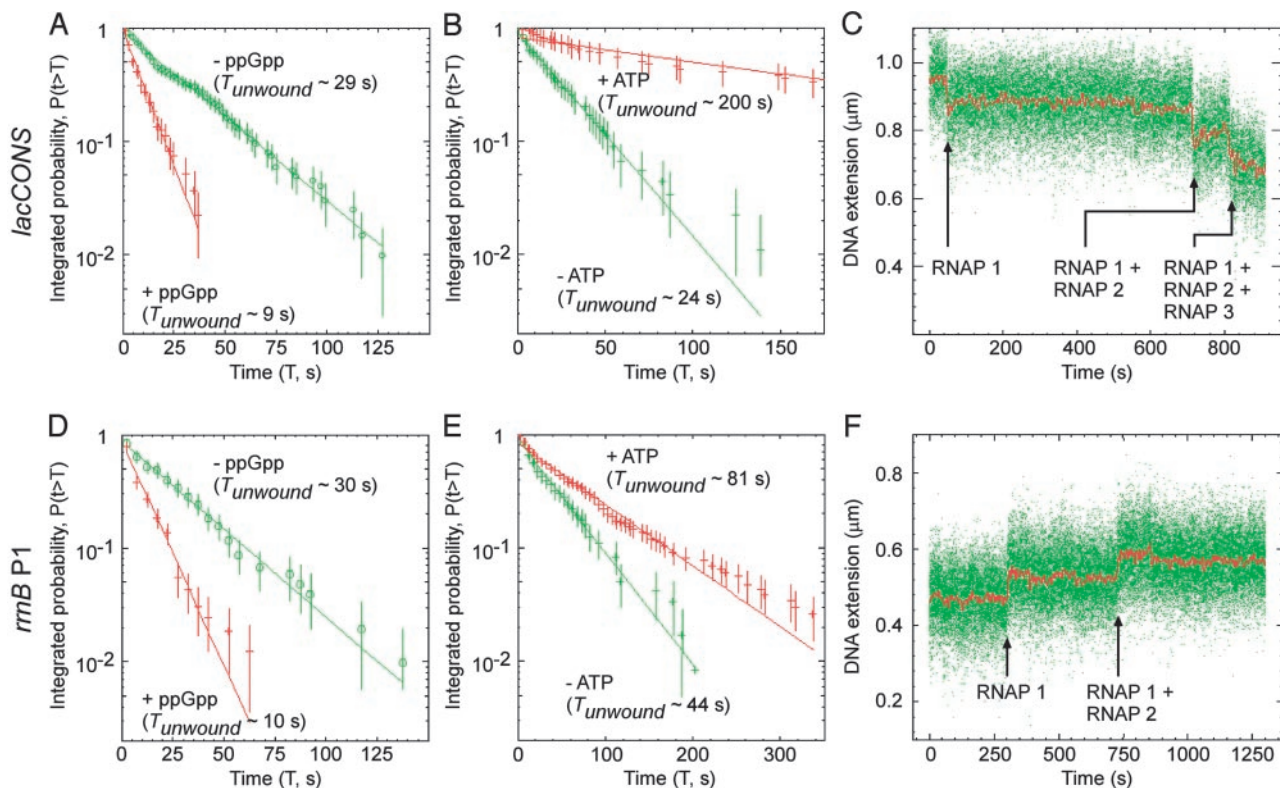

Fig. 4. Effects of ppGpp, effects of initiating nucleotide, and observation of promoter clearance. (*A*) Effects of ppGpp (0 or 100 μM) on stability of the unwound complex (consensus promoter, positively supercoiled DNA; $\sigma = 0.018$; $n = 200$ events). (*B*) Effects of ATP (0 or 2 mM) on stability of the unwound complex (consensus promoter, positively supercoiled DNA; $\sigma = 0.018$; $n = 100$ events). (*C*) Observation of promoter clearance by detection of successive, cumulative unwinding events, each corresponding to promoter clearance by RNAP molecule *n*, followed by promoter binding and unwinding by RNAP molecule *n* + 1 (consensus promoter, positively supercoiled DNA; 2 mM each NTP). (*D*–*F*) As in *A*–*C*, but for the *rrnB* P1 promoter, with negatively supercoiled DNA.

To assess effects of promoter sequence, we performed parallel experiments with the *rrnB* P1 promoter, which, based on the literature, forms exceptionally unstable, reversible open complexes (23). Fig. 2D documents that, with negatively supercoiled DNA, the *rrnB* P1 promoter exhibits unstable, reversible unwinding ($T_{unwound}$ = 16 s; compare $T_{unwound}$ > 10,000 s for the consensus promoter). Fig. 2E documents that, with positively supercoiled DNA, the *rrnB* P1 promoter exhibits no detectable unwinding ($T_{unwound}$ = 0 s; compare $T_{unwound}$ = 34 s for the consensus promoter). The transition amplitude for promoter unwinding at the *rrnB* P1 promoter is indistinguishable from that at the consensus promoter ($\Delta l_{obs,neg}$ = 50 ± 5 nm vs. $\Delta l_{obs,neg}$ = 50 ± 5 nm; Fig. 2 A, B, and D), suggesting that the extents of unwinding and the extents of compaction at the two promoters are identical.

The effector ppGpp and initiating nucleotides have been reported to have significant effects on the stability of the open complex (24, 25). Fig. 4 A and B document effects of ppGpp on the stability of the unwound complex at, respectively, the consensus promoter and the *rrnB* P1 promoter. At both promoters, addition of ppGpp results in a large ($\approx$3-fold) decrease in the lifetime of the unwound complex, in quantitative agreement with expectation based on the literature (24). Fig. 4 C and D documents effects of initiating nucleotides on the stability of the unwound complex at, respectively, the consensus promoter and the *rrnB* P1 promoter. At the consensus promoter, where ATP is able to serve as both the initiating nucleotide and the second nucleotide (permitting synthesis of the dinucleotide pppApA), addition of ATP results in a large ($\approx$10-fold) increase in $T_{unwound}$. At the *rrnB* P1 promoter, where ATP is able to serve as the initiating nucleotide but not as the second nucleotide, addition of ATP results in a moderate, but reproducible ($\approx$2-fold), increase in $T_{unwound}$. Control experiments show that the effects are nucleotide-specific. Thus, addition of the noncomplementary nucleotide GTP results in no increase in $T_{unwound}$, neither at the consensus promoter nor at the *rrnB* P1 promoter (data not shown). We conclude that initiating nucleotides stabilize the unwound complex, consistent with expectation based on the literature (25).

To demonstrate that our experimental approach also can detect promoter clearance, we performed experiments in the presence of all four nucleoside triphosphates (NTPs) (ATP, CTP, GTP, and UTP). The rationale is as follows: in the presence of all four NTPs, RNAP molecule *1* will bind and unwind the promoter (just as in the absence of NTPs); after an interval of time (T_{clear}), RNAP molecule *1* will clear the promoter, rendering the promoter accessible, and permitting RNAP molecule 2 to bind and unwind, yielding a second, cumulative unwinding event; and so forth. Thus, by this logic, experiments in the presence of all four NTPs should yield successive, cumulative unwinding events, with each successive, cumulative unwinding event reporting promoter clearance by RNAP molecule *n*, followed by promoter binding and unwinding by RNAP molecule *n* + 1. Fig. 4 E and F shows that precisely such patterns of successive, cumulative unwinding events are observed, with both the consensus promoter (with positively supercoiled DNA) and the *rrnB* P1 promoter (with negatively supercoiled DNA). Extensive control experiments establish that the observed successive, cumulative unwinding events in fact reflect promoter clearances by RNA polymerase *n* and binding and unwinding by RNA polymerase molecule *n* + 1 (data not shown). In principle, the experimental time traces for each successive, cumulative unwinding event yields three observables relevant to the mechanism and kinetics of promoter clearance: (*i*) the number of states in the event (which reflects the number of unwinding intermediates in promoter clearance); (*ii*) the transition amplitude of the event (which reflects the extent of DNA unwinding and extent of DNA compaction in promoter clearance and permits determination of the extent of unwinding and extent of compaction in the transcription elongation complex); and (*iii*) the time interval between events (which reflects T_{clear} + T_{wait} and permits determination of the kinetics of promoter clearance). Further experiments will be essential to realize the full potential of the approach for analysis of promoter clearance.

Our approach and results provide a single-molecule study of transcription initiation.

We note that our approach should be generalizable to analysis of other nucleic-acid-processing factors that affect DNA twist and/or DNA compaction. Integration of our approach (which permits control and readout of DNA torsional state) with single-molecule fluorescence (which permits readout of binding, translocation, and conformational states) should provide unprecedented opportunities for structural, mechanistic, and kinetic analysis of nucleic-acid-processing factors.

1. Record, M. T. J., Reznikoff, W., Craig, M., McQuade, K. & Schlax, P. (1996) in *Escherichia coli and Salmonella*, ed. Neidhart, F. C. (Am. Soc. Microbiol. Press, Washington, DC), Vol. 1, pp. 792–820.
2. deHaseth, P., Zupancic, M. & Record, M. T. J. (1998) *J. Bacteriol.* **180,** 3019–3025.
3. Strick, T., Allemand, J., Bensimon, D., Bensimon, A. & Croquette, V. (1996) *Science* **271,** 1835–1837.
4. Strick, T., Allemand, J.-F., Bensimon, D. & Croquette, V. (1998) *Biophys. J.* **74,** 2016–2028.
5. Revyakin, A., Allemand, J.-F., Croquette, V., Ebright, R. & Strick, T. (2003) *Methods Enzymol.* **370,** 577–598.
6. White, J. (1969) *J. Math.* **91,** 693–728.
7. Mukhopadhyay, J., Kapanidis, A., Mekler, V., Kortkhonjia, E., Ebright, Y. & Ebright, R. (2001) *Cell* **106,** 453–463.
8. Mekler, V., Kortkhonjia, E., Mukhopadhyay, J., Knight, J., Revyakin, A., Kapanidis, A., Niu, W., Ebright, Y., Levy, R. & Ebright, R. (2002) *Cell* **108,** 599–614.
9. Cech, C. & McClure, W. (1980) *Biochemistry* **19,** 2440–2447.
10. Zaychikov, E., Denissova, L., Meier, T., Gotte, M. & Heumann, H. (1997) *J. Biol. Chem.* **272,** 2259–2267.
11. Rivetti, C., Guthold, M. & Bustamante, C. (1999) *EMBO J.* **18,** 4464–4475.
12. Naryshkin, N., Revyakin, A., Kim, Y., Mekler, V. & Ebright, R. (2000) *Cell* **101,** 601–611.
13. McClure, W. (1980) *Proc. Natl. Acad. Sci. USA* **77,** 5634–5638.
14. Malan, T. P., Kolb, A., Buc, H. & McClure, W. (1984) *J. Mol. Biol.* **180,** 881–909.
15. Amouyal, M. & Buc, H. (1987) *J. Mol. Biol.* **195,** 795–808.
16. Borowiec, J. & Gralla, J. D. (1987) *J. Mol. Biol.* **195,** 89–97.
17. Su, T. T. & McClure, W. R. (1994) *J. Biol. Chem.* **269,** 13511–13521.
18. Strick, T., Allemand, J.-F., Bensimon, D. & Croquette, V. (2000) *Annu. Rev. Biophys. Biomol. Struct.* **29,** 523–543.
19. ten Heggeler-Bordier, B., Wahli, W., Adrian, M., Stasiak, A. & Dubochet, J. (1992) *EMBO J.* **11,** 667–672.
20. Lavigne, M., Kolb, A., Yeramian, E. & Buc, H. (1994) *EMBO J.* **13,** 4983–4990.
21. Strick, T., Bensimon, D. & Croquette, V. (1999) *Genetica* **106,** 57–62.
22. Kanaar, R. & Cozzarelli, N. (1992) *Curr. Opin. Struct. Biol.* **2,** 369–379.
23. Gourse, R. (1988) *Nucleic Acids Res.* **16,** 9789–9809.
24. Barker, M., Gaal, T., Josaitis, C. & Gourse, R. (2001) *J. Mol. Biol.* **305,** 673–688.
25. Gaal, T., Bartlett, M., Ross, W., Turnbough, C. & Gourse, R. (1997) *Science* **278,** 2092–2097.
26. Rief, M., Fernandez, J. & Gaub, H. (1998) *Phys. Rev. Lett.* **81,** 4765–4767.